ELSEVIER

Journal of Applied Geophysics 50 (2002) 401–416

JOURNAL OF APPLIED GEOPHYSICS

www.elsevier.com/locate/jappgeo

Generalised Series Expansion (GSE) used in DC geoelectric–seismic joint inversion

Márta Kis *

Geodetic and Geophysical Research Institute of the Hungarian Academy of Sciences, P.O. Box 5, H-9401 Sopron, Hungary

Received 18 October 1999; accepted 16 May 2002

Abstract

Horizontally layered (1D) earth models are often assumed as a model estimate for the interpretation of geophysical data measured along 2D geological structures. In this process, the individual data sets are usually inverted independently, and it is considered only in a later phase of interpretation that these local (1D) models have common characteristic features. Taking account of these common attributes, instead of the successive independent interpretations, the lateral variations of geometrical and petrophysical parameters can be efficiently determined for the whole 2D structure by applying a series expansion. Using global basis functions, two advantages can be achieved: (i) choosing an appropriate number of basis functions helps us to restrict the complexity of the model; (ii) the integration of all the data sets measured along the profile gives rise to the application of simultaneous or joint inversion methods. This results in a decrease of the number of independent unknowns, a higher stability during the inversion and a more accurate and reliable parameter estimation. In this paper, a joint inversion algorithm is presented using DC geoelectric apparent resistivities and refraction seismic travel times measured along various layouts above a 2D geological model. To describe lateral variations series, expansions are used, and furthermore, to improve the often used approximation of a (locally) 1D forward modelling, the integral mean value of the horizontally changing model parameters (calculated along an appropriately defined interval) is introduced. We call the inversion procedure that combines series expansions and the concept of integral mean Generalised Series Expansion (GSE) inversion. The method was developed and tested for both the simultaneous (integrating data sets of one method or methods on the same physical basis) and the joint inversion (where data sets of methods on different physical bases are joined together), using synthetic and field data sets. It is also demonstrated that the equivalence problem inherent in the independent inversion of DC geoelectric data can efficiently be resolved by the use of the joint GSE inversion method in the cases of conductive and resistive equivalent geological models.

Keywords: Two-dimensional model; Inversion algorithm; Joint inversion; Simultaneous inversion; Equivalence

1. Introduction

Geophysical data are often interpreted assuming horizontally layered geologic models. Beard and Morgan (1991) demonstrated that 1D inversion can provide acceptable estimates in constructing contoured cross sections in case of significant 2D subsurface structures. The 1D geoelectric inversion often has internal nonuniqueness and ambiguity problems (Koefoed, 1979). To reduce these difficulties, various regularization procedures are used (Lines and Treitel, 1984, Tarantola, 1987). An efficient way to overcome internal ambiguities is the use of the joint inversion,

* Fax: +36-99-508-355.
E-mail address: m_kis@ggki.hu (M. Kis).

0926-9851/02/$ - see front matter
PII: S0926-9851(02)00167-2

which means the integration of various groups of data records (arising from physically or geometrically different methods and surveys) into a single inversion algorithm. The joint inversion algorithm was introduced by Vozoff and Jupp (1975) for magnetotelluric (MT) and DC resistivity data and extensively studied, e.g. by Yang and Tong (1988) and Dobróka et al. (1991), who integrated DC geoelectric and VSP data, and Hering et al. (1995). Kis et al. (1995) proposed a joint inversion method for the interpretation of seismic surface wave dispersion, refraction and DC geoelectric data. Joint inversion based on global optimization was also applied by Kis (1996, 1998, pp. 51–73) for 1D DC resistivity and refraction seismic data, and Sharma and Kaikkonen (1999) for 1D EM and DC measurements.

Instead of the independent (1D) interpretation of geophysical data measured with different layouts above an approximately 2D structure, the lateral variations of geometrical and petrophysical parameters (such as resistivities, velocities and densities) can efficiently be determined by combining series expansion methods and (simultaneous or joint) inversion algorithms. The advantages of the Series Expansion (SE) inversion were demonstrated by Dobróka (1994), who applied the Wentzel–Kramer–Brillouin (WKB) solutions (Morse and Feschbach, 1953) for the interpretation of seismic dispersion data for 2D structures, using a 1D approximation in the forward modelling. The inversion was formulated for the coefficients of a series expansion, where power functions and cell-wise constant functions were applied as basis functions.

Gyulai and Ormos (1997, 1999) developed a simultaneous SE inversion of DC sounding curves with power and periodical basis functions (called 1.5D inversion), Kis (1998, pp. 73–99) applied simultaneous and joint SE inversion for the interpretation of DC geoelectric and seismic refraction data, pointing out and examining the improvement possibility of the approximate 1D forward modelling applied in SE inversion methods, introducing the integral mean concept to the SE inversion. Simultaneous and joint SE inversion were also applied by Ormos et al. (1998), Kis et al. (1999, 2001), Dobróka et al. (2001) and Török and Kis (2001) for the interpretation of geoelectric and seismic data.

In this paper, DC geoelectric apparent resistivities and refraction seismic travel times measured along various lines parallel to the strike direction of the 2D geologic model are integrated into a joint inversion algorithm. To describe the variation of the geometrical and petrophysical parameters, a series expansion method is used. In our approach, we introduced the integral mean of these functions calculated for an appropriately chosen interval instead of the local values of the functions expressing the lateral change of thickness and petrophysical parameters, respectively. These laterally averaged quantities serve as model parameters in the 1D forward modelling. We call the inversion method, which applies series expansion in combination with the concept of integral mean, Generalised Series Expansion (GSE) method. In our investigations, Chebyshev polynomials and interval-wise constant functions are used as basis functions. The algorithm was constructed for both the simultaneous and the joint inversion versions and tested using synthetic and field data sets. It is also demonstrated that the equivalence problem of the DC geoelectric inversion can efficiently be resolved by the use of the joint GSE method.

2. Simultaneous and joint SE (and GSE) inversion

In order to expand the Generalised Series Expansion (GSE) method, we used the notation in Fig. 1, where the measurement layout is shown. The x-axis of a Cartesian coordinate system is directed parallel to the dip direction, while the measurement lines are in the strike direction. In this case, the thickness and the petrophysical parameters are functions of the x and z coordinates only. We solved the 2D inverse problem using the data of all layouts.

As an example, let us consider the thickness of the ith layer below the jth measurement line. In 1D forward modelling, it is reasonable to define it as the local value of the $h_i(x)$ thickness function at the point $x=x_j$,

$$h_i^{(j)} = h_i(x_j), \tag{1}$$

as it is considered in the SE algorithm (Gyulai and Ormos, 1997, 1999).The thickness functions and the petrophysical parameters are to be discretized. Let us assume $\Phi_k(x)$ to be a (usually orthogonal) set of basis

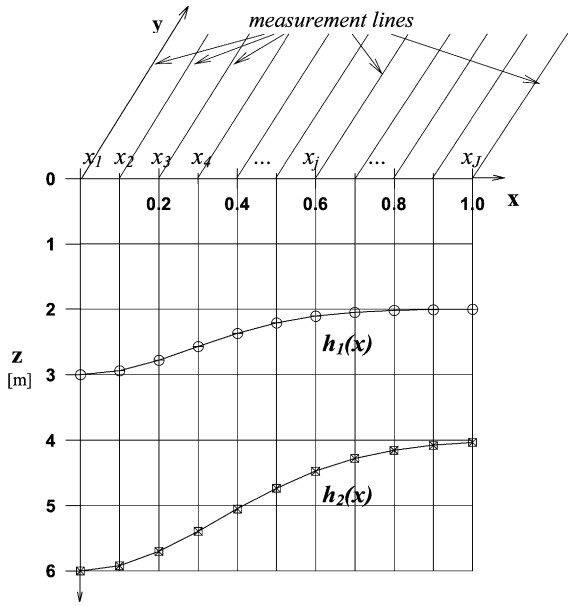

Fig. 1. The model and layouts assumed in the GSE inversion.

function of a series expansion and, for instance, write the thicknesses in the form of the series expansion

$$h_i(x) = \sum_{k=1}^{K_{h,i}} B_i^{(k)} \Phi_k(x), \tag{2}$$

where $B_i^{(k)}$'s are the expansion coefficients and $K_{h,i}$ are the number of coefficients for the thickness functions.

On the other hand, it is obvious that not only the local thickness beneath the x_j coordinate (Eq. (1)) participate in determining the data set measured along the measurement line positioned at x_j but all the thickness within a certain interval around this x_j coordinate. Because of this, in order to improve the SE algorithm using the 1D approximation where the series expansion is formulated for the local thickness values, we substituted the actual thickness with the integral mean

$$\hat{h}_i^{(j)} = \frac{1}{2\Delta} \int_{x_j-\Delta}^{x_j+\Delta} h_i(x)\mathrm{d}x, \tag{3}$$

where Δ is an appropriately chosen distance defined along the x-axis.

This approach serves for providing a more complete "lateral sight" for the GSE method incorporating the lateral parameter changes, in spite of applying the 1D approximation in the forward modelling. It is also obvious that in the course of application the GSE algorithm is capable of giving back the SE method by choosing the extreme case of $\Delta \to 0$.

Formulating the series expansion (Eq. (2)) for the integral mean thickness (Eq. (3)), it can be written as

$$\hat{h}_i^{(j)} = \sum_{k=1}^{K_{h,i}} B_i^{(k)} S_{k,j}, \tag{4}$$

where

$$S_{k,j} = \frac{1}{2\Delta} \int_{x_j-\Delta}^{x_j+\Delta} \Phi_k(x)\mathrm{d}x. \tag{5}$$

In the following, we expanded the joint inversion algorithm called Generalised Series Expansion (GSE) method, which is based on the combination of the series expansion and the integral mean formulae. Besides the improvement, the GSE inversion method keeps the advantage of the SE algorithm, namely that the (mean) thicknesses along all the measurement lines are expressed by the same expansion coefficients. This results in a reduction of the number of independent unknowns (relative to the number of data) and a higher stability in the inversion.

The basic assumption of the GSE inversion algorithm is that 1D calculations are used for the forward modelling (using the mean model parameters) but the unknowns are the expansion coefficients of thickness functions (representing the whole 2D variation of boundaries) as well as the petrophysical parameters (assumed to be laterally constant at this step of constructing the algorithm).

In the present study, the lines along which the geoelectric and seismic measurements have been carried out are parallel to the strike direction of the model. The method needs further improvement in the future, e.g. for the two-variable (superficial) series expansion or combined application of regularisation equations (Gyulai, 2000) in order to be applicable for the more common case of layout directions, e.g. being parallel to the profile direction.

The flowchart of the algorithm is presented in Fig. 2. In this approach, if all the different data sets are integrated in the joint GSE inversion, the combined calculated and measured data vectors are given as

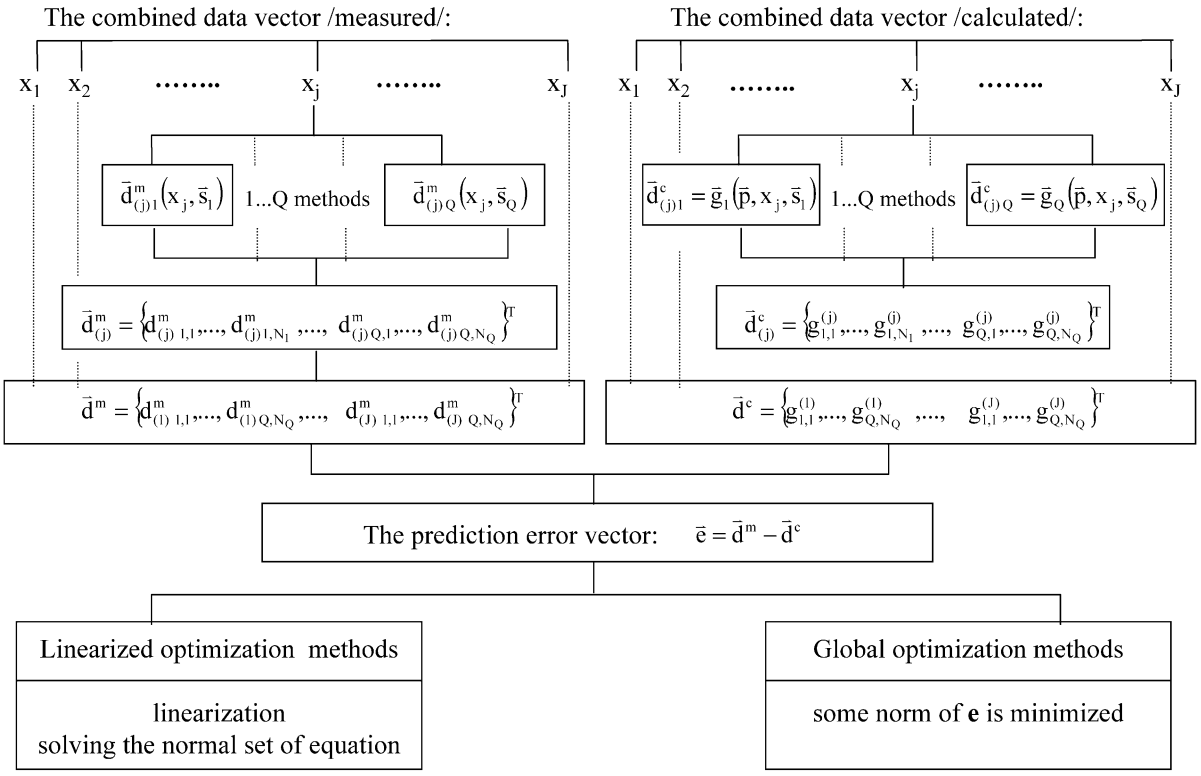

Fig. 2. The simultaneous and joint SE/GSE inversion algorithm.

follows. Let us denote the calculated data vector ($\vec{d}^{c}_{(j)q}$) as

$$\vec{d}^{c}_{(j)q} = \vec{g}_q(\vec{p}, x_j, \vec{s_q}), \qquad (q = 1, \ldots, Q), \tag{6}$$

and the measured data vector ($\vec{d}^{m}_{(j)q}$) belonging to the qth geophysical method at the measurement line placed at the coordinate x_j. $\vec{s_q}$ denotes the positional parameter of the datum, e.g. $s_{1,k}(AB/2)_k$ in case of the kth VES data (in case $q=1$), and $s_{2,k}=r_k$, the source-geophone distance in case of refraction seismics ($q=2$). Q is the number of the methods involved in the joint inversion.

In the case that all the data integrated in the inversion procedure are of the same physical nature ($Q=1$), we speak of simultaneous GSE inversion.

Integrating the data measured by all the Q methods at a certain x_j, the combined data vector is to be defined as

$$\vec{d}^{c}_{(j)} = \{g^{(j)}_{1,1}, \ldots, g^{(j)}_{1,N_1}, \ldots, g^{(j)}_{Q,1}, \ldots, g^{(j)}_{Q,N_Q}\}^{T}, \tag{7}$$

similarly to Dobróka et al. (1991). In case of GSE joint inversion, the data sets represented in Eq. (7) are ordered in the sequence of $j=1,\ldots,J$ as

$$\vec{d}^{c} = \{g^{(1)}_{1,1}, \ldots, g^{(1)}_{Q,N_Q}, \ldots, g^{(J)}_{1,1}, \ldots, g^{(J)}_{Q,N_Q}\}^{T}. \tag{8}$$

The same form is applied for the measured data:

$$\vec{d}^{m} = \{d^{(1)}_{1,1}, \ldots, d^{(1)}_{Q,N_Q}, \ldots, d^{(J)}_{1,1}, \ldots, d^{(J)}_{Q,N_Q}\}^{T}. \tag{9}$$

In order to construct the joint inversion algorithm, we have to introduce the combined parameter vector, which must contain the local or integrated parameters or simply the expansion coefficients, which represents the functions of parameters. For instance, combining the DC geoelectric sounding (VES) and seismic refraction methods, we get:

$$\vec{p} = \{\hat{h}^{(1)}_1, \ldots, \hat{h}^{(1)}_{n-1}, \ldots, \hat{h}^{(J)}_1, \ldots, \hat{h}^{(J)}_{n-1}, \rho_1, \ldots, \rho_n, v_{p1}, \ldots, v_{pn}\}^{T}, \tag{10}$$

where ρ_i, and v_{pi} are the resistivity values and the velocity of longitudinal waves for the ith layer ($i=1,\ldots,n$), respectively, which are assumed to be laterally constant at this step.

If we assume a more general geologic case in which the model is laterally (weakly) inhomogeneous, the GSE parameter vector should also be modified. Expanding the resistivity function $\rho(x)$ in terms of the same Φ_k basis function as in Eq. (2), we find

$$\rho_i(x) = \sum_{k=1}^{K_\rho} B_i^{(k+K_h)} \Phi_k(x). \tag{11}$$

Using the integral mean as a more realistic approximation in 1D forward modelling, we can introduce the local (mean) resistivity at $x=x_j$ as

$$\hat{\rho}_i^{(j)} = \sum_{k=1}^{K_\rho} B_i^{(k+K_h)} S_{k,j}, \tag{12}$$

where $S_{k,j}$ is given in Eq. (5). Similarly, assuming a laterally (weakly) varying P-velocity ($v_p(x)$), we can write

$$\hat{v}_{pi}^{(j)} = \sum_{k=1}^{K_\alpha} B_i^{(k+K_h+K_\rho)} S_{k,j}. \tag{13}$$

The more general parameter vector combined for joint GSE inversion can similarly be written as

$$\begin{aligned}\overrightarrow{p} = \{&B_1^{(1)},\ldots,B_1^{(K_h)},\ldots,B_{n-1}^{(1)},\ldots,B_{n-1}^{(K_h)},\ldots,\\ &B_1^{(K_h+1)},\ldots,B_1^{(K_h+K_\rho)},\ldots,B_n^{(K_h+1)},\ldots,B_n^{(K_h+K_\rho)},\ldots,\\ &B_1^{(K_h+K_\rho+1)},\ldots,B_1^{(K_h+K_\rho+K_\alpha)},\ldots,B_n^{(K_h+K_\rho+1)},\ldots,\\ &B_n^{(K_h+K_\rho+K_\alpha)}\}^{\mathrm{T}}.\end{aligned} \tag{14}$$

The calculated data given in Eq. (8) are nonlinear functions of the elements of the model parameter vector (Eq. (14)). Using global optimization methods, we search for a solution by minimizing directly a certain norm of the prediction error vector $\overrightarrow{e} = \overrightarrow{d}^{\mathrm{m}} - \overrightarrow{d}^{\mathrm{c}}$.

If one tries to use the faster linearized methods, the function expressing the connection between the calculated data and the model parameters need to be approximated by its Taylor series truncated at the linear term. Minimizing the L_2 norm of the normalized prediction error vector $\boldsymbol{f}_i = y_i - \sum_{k=1}^{M} G_{ik}x_k$, one can get the normal equation

$$\underline{\underline{G}}^{\mathrm{T}}\underline{\underline{G}}\overrightarrow{x} = \underline{\underline{G}}^{\mathrm{T}}\overrightarrow{y}, \tag{15}$$

where

$$\begin{aligned} y_i &= \frac{d_i^{\mathrm{m}} - d_i^{(0)}}{d_i^{\mathrm{m}}},\ x_k = \frac{\delta P_k}{p_k^{(0)}},\\ G_{ik} &= \frac{p_k^{(0)}}{d_i^{\mathrm{m}}}\left(\frac{\partial d_i^{\mathrm{c}}}{\partial p_k}\right)\Bigg|_{\overrightarrow{p}=\overrightarrow{p}^{(0)}},\ \delta P_k = (p_k - p_k^{(0)}) \end{aligned} \tag{16}$$

and $\overrightarrow{p}^{(0)}$ is an initial estimate of the parameter vector as it is often used (Dobróka et al., 1991). In the relative prediction error vector $\boldsymbol{f}$, the deviation of data (y_i) and parameters (x_k) are normalized after the magnitudes of data and parameters participating in the inversion. Applying this normalized equation set based on $\boldsymbol{f}$, one can avoid the biasing effect of the different orders of magnitudes of data that should be handled together during the joint inversion. In the following investigations, the algorithm will be tested in the faster linearized version.

The choice of the basis functions (Eq. (2)) mainly depends on the geologic model, which usually requires prior knowledge. In this paper, we apply two specific kinds of basis functions, the Chebyshev polynomials of the kth order ($T_k(x)$) and interval-wise constant functions defined as

$$\Phi_j(x) = \begin{cases} 1, & \text{if } x \in V_j \\ 0, & \text{if } x \notin V_j \end{cases} \tag{17}$$

where V_j denotes an interval around the point $x=x_j$.

3. Numerical investigations

In order to test the reliability and accuracy of the GSE inversion method, we used synthetic and field data sets. In this paper, data of the seismic refraction and DC geoelectric sounding (VES) methods are integrated in the GSE inversion process.

For the generation of synthetic data, we defined a two-dimensional model, shown in Fig. 1, where:

$$h_1(x) = 2 + \mathrm{e}^{-(2.5x)^2}, \tag{18}$$

$$h_2(x) = 4 + 2\mathrm{e}^{-(2x)^2}. \tag{19}$$

The petrophysical parameters given in Table 1 are independent of x.

Table 1
The parameters of the exact model used in the numerical test

i	ρ [Ω m]	v_p [m/s]
1	25	700
2	50	1500
3	100	2300

For simplicity, the x coordinates are transformed to the interval of $[-1,1]$. The geoelectric data are calculated in a Schlumberger array for 30 logarithmically equidistant points from 0.5 to 300 m. The refraction travel times are generated for 50 geophone arrays assuming equidistant geophone layouts with 5 m distance between the source and first receiver and 1.5 m between the neighbouring ones.

Theoretical data were calculated by using 2D and 3D finite difference forward codes, for which I wish to express my special thanks to Dr. Á. Gyulai, Dr. T. Ormos, E. Prácser (Eötvös Loránd Geophysical Institute) and Ms. I. Török. The data are contaminated by 1% random noise.

3.1. Results based on the use of interval-wise constant functions

We start our investigations with the special case of the GSE method, using the interval-wise constant functions as basis functions. This particular case provides the opportunity that the expansion coefficients, given by the GSE inversion, can be directly interpreted as the local thicknesses of the layers (Eq. (4)). Accordingly, the covariance matrix $\underline{\mathrm{COV}}(\vec{p}) = \sigma^2(\underline{G}^{\mathrm{T}}\underline{G})^{-1}$, where σ^2 is the variance of the data (Menke, 1984), also has a direct meaning; its elements characterize the reliability of the direct petrophysical and geometrical parameters ($\vec{p}$) of the problem.

Numerical tests were carried out to investigate how the accuracy and reliability of the GSE parameter estimation depend on the number of measurement lines in the cases using a single VES method and jointly using the refraction seismic method with VES.

In order to quantify the accuracy of data fitting of the different procedures used in the numerical investigations, the relative data distance E

$$E = \sqrt{\frac{1}{N}\sum_{j=1}^{N}\left(\frac{d_j^{\mathrm{m}} - d_j^{\mathrm{c}}}{d_j^{\mathrm{m}}}\right)^2} \qquad (20)$$

is used, where N is the number of data. To characterize the accuracy of the parameter estimation, we use the relative model distance D

$$D = \sqrt{\frac{1}{M}\sum_{j=1}^{M}\left(\frac{p_j^{\mathrm{exact}} - p_j^{\mathrm{estimated}}}{p_j^{\mathrm{exact}}}\right)^2} \times 100\% \qquad (21)$$

(Dobróka et al., 1991), and D_h, calculated for the local thickness beneath the measurement lines

$$D_h = \sqrt{\frac{1}{N_h}\sum_{i=1}^{N_h}\left(\frac{h_i^{\mathrm{exact}} - h_i^{\mathrm{estimated}}}{h_i^{\mathrm{exact}}}\right)^2} \times 100\%, \qquad (22)$$

where M is the number of the model parameters and N_h is the number of the local thickness. In order to quantify the reliability of the parameter estimation,we used the mean variance MV

$$\mathrm{MV} = \sqrt{\frac{1}{M}\sum_{i=1}^{M}\mathrm{COV}_{ii}} \qquad (23)$$

(COV_{ii} denotes the parameter variances, Menke, 1984), and the correlation norm T, defined as

$$T = \sqrt{\frac{1}{M(M-1)}\sum_{i=1}^{M}\sum_{j=1}^{M}\left(\mathrm{CORR}_{ij} - \delta_{ij}\right)^2}, \qquad (24)$$

where CORR denotes the correlation matrix,

$$\mathrm{CORR}_{ij} = \frac{\mathrm{COV}_{ij}}{\sqrt{\mathrm{COV}_{ii}\mathrm{COV}_{jj}}}, \qquad (25)$$

and δ_{ij} is the Kronecker symbol.

In Fig. 3a–d, the results concerning the different numbers of measurement lines are shown, for the cases of the simultaneous (geoelectric VES) and the joint (refraction seismic–geoelectric) inversion.

The results demonstrated that increasing the number of measurement lines (J) involved in the simultaneous or joint GSE inversion, the quantities D and D_h (characterizing the distance in the model space, or the accurate fitting between the exact and estimated values of the model parameters) monotonically decrease, demonstrating a definite improvement in

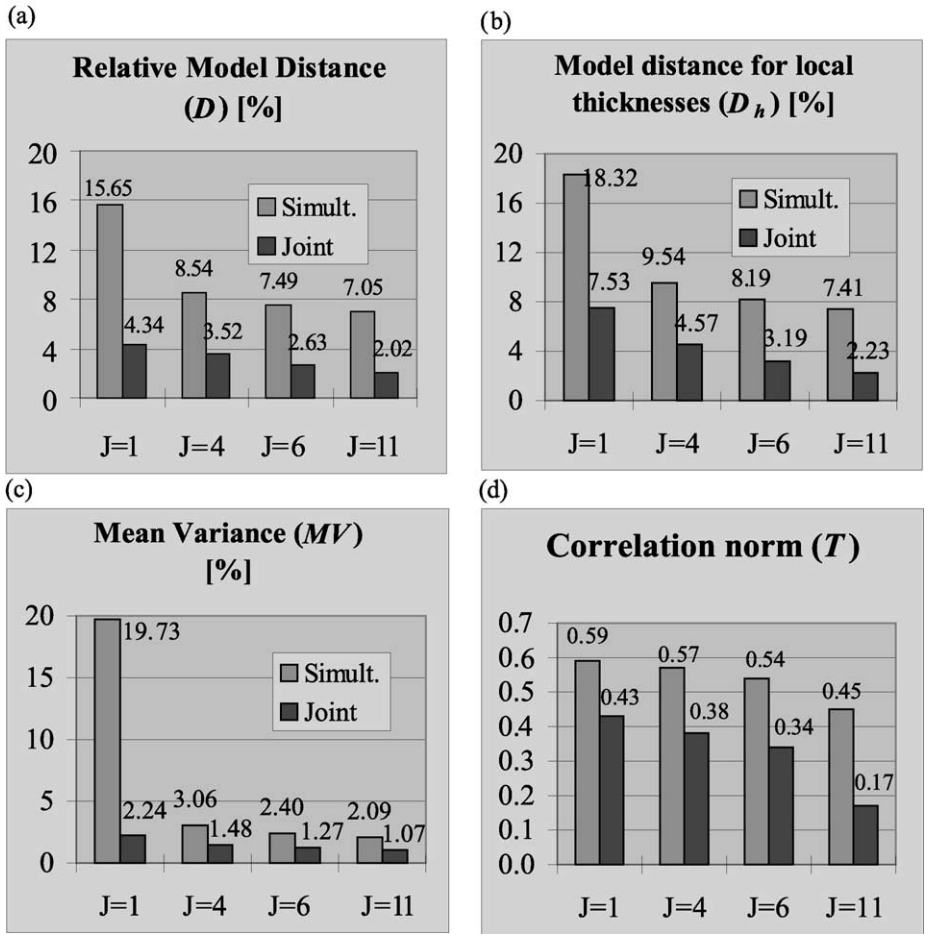

Fig. 3. (a–d) The qualifying results of the simultaneous and the joint GSE inversion in the function of the number of the measurement lines (J).

the accuracy of parameter estimation. The same tendency can be observed for MV and T qualifying the estimation of the inversion, which indicates a more reliable parameter estimation.

As an example, for $J=7$, the exact thickness functions are given by solid lines in Fig. 4, while the estimated local thicknesses based on the simultaneous inversion and on the joint inversion are given by squares and circles, respectively.

3.2. Results based on Chebyshev polynomials

Chebyshev polynomials are often used in geophysical applications. Their use has also appreciable numerical advantage in the framework of the GSE method. Here, the basis functions will be defined as Chebyshev polynomials and the set of equidistant integration intervals will be chosen to cover the whole range of interest along the x direction without overlapping. In our numerical test, we assumed three kinds of measurement arrays with $J=21$, $J=11$ and $J=7$ measurement lines.

As a first step, we tested the discretization error of the GSE method. We generated a noise-free VES data and reconstructed the thickness functions of the geological model. The results are given in Fig. 5 at various orders (P) of the Chebyshev polynomials. As it is shown, the GSE inversion is unacceptably inaccurate below the order $P=4$ even in the case of noise-free data. So in the later tests, we use Cheby-

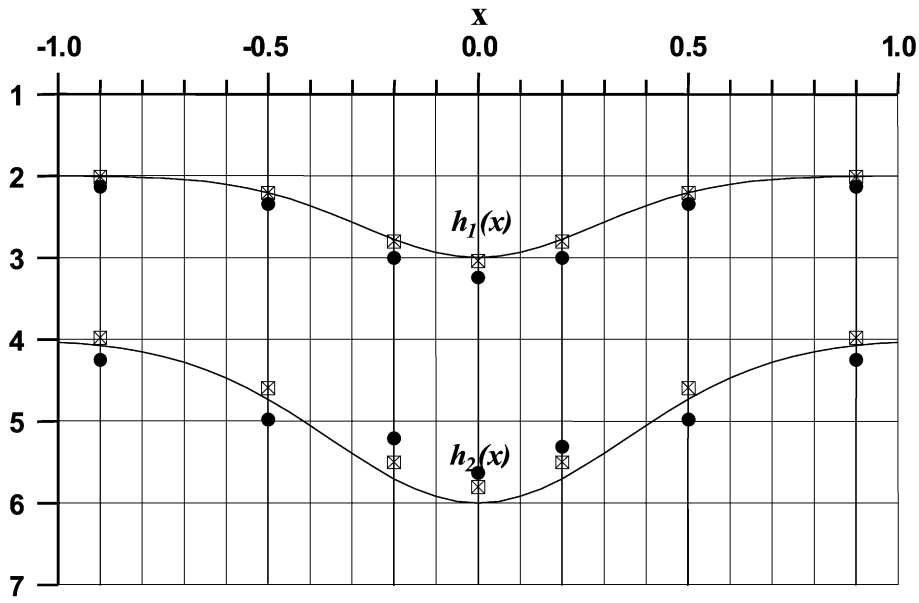

Fig. 4. The results of the simultaneous (rectangles) and joint (circles) GSE inversion based on interval-wise constant functions ($J=7$).

shev polynomials of order $P=5$ and $P=7$. We must note that choosing an appropriate order (P) has great importance as the higher order the better fit we have, but at the same time, the number of the unknowns is increased comparing to the number of measurement lines (J).

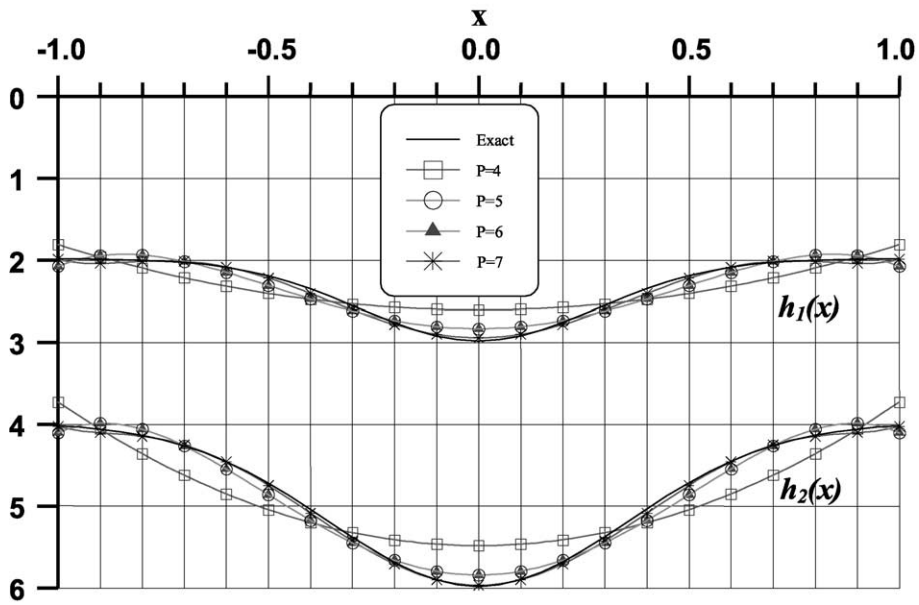

Fig. 5. The discretization error when Chebyshev polynomials are used in the approximation of the depth functions (P is the order of the polynomials).

In order to characterize the reconstruction accuracy of the thickness functions, we introduced:

$$D_f = \sqrt{\frac{1}{N_f(n-1)}\sum_{j=1}^{n-1}\sum_{i=1}^{N_f}\left(\frac{h_j^{\text{exact}}(x_i) - h_j^{\text{estimated}}(x_i)}{h_j^{\text{exact}}(x_i)}\right)^2} \times 100\%, \quad (26)$$

where

$$x_i = -1 + (i-1)\frac{2}{(N_f - 1)},$$

n is the number of layers and N_f is a sufficiently large integer ($N_f = 101$ in our investigations). The quantity

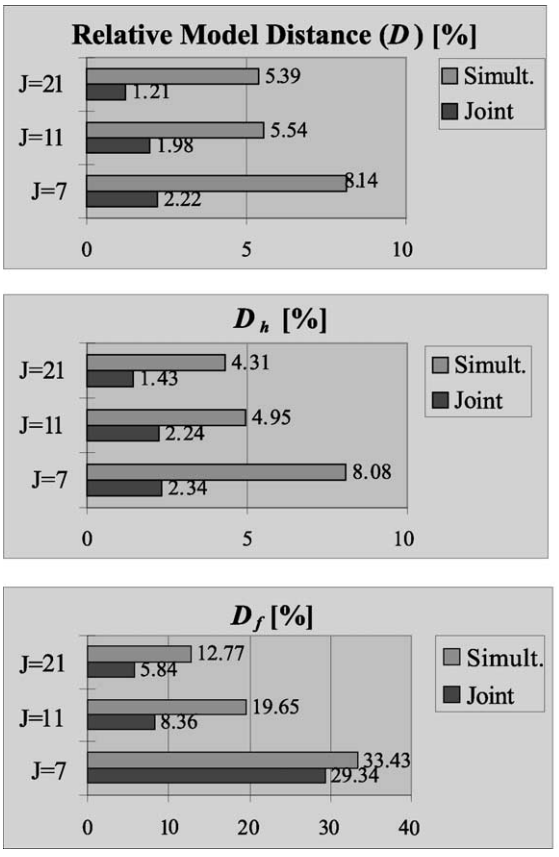

Fig. 6. The results of the simultaneous and joint GSE inversion at various number of measurement lines (polynomial order is $P = 7$).

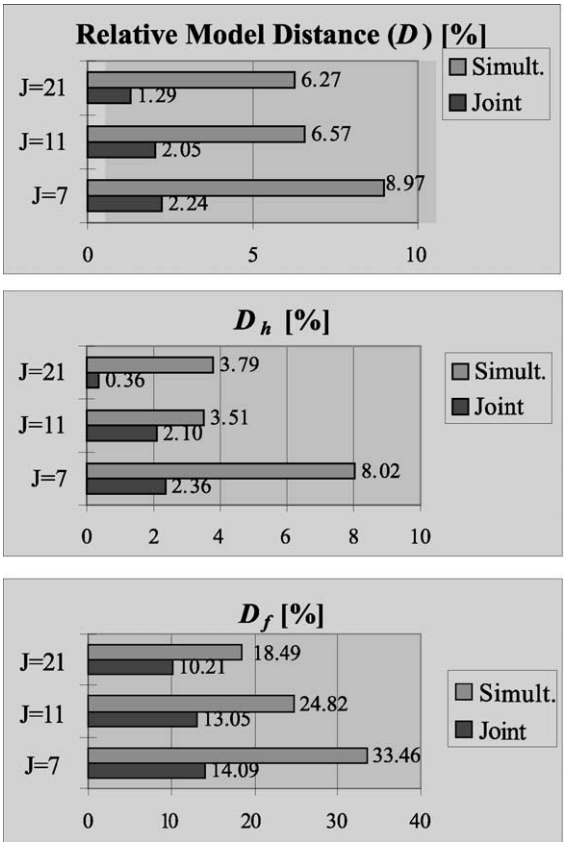

Fig. 7. The results of the simultaneous and joint GSE inversion at various number of measurement lines (polynomial order is $P = 5$).

D_f serves to measure the relative distance between the exact and the estimated thickness functions along the whole interval $(-1,1)$ and not only at points at which the measurement lines are positioned.

Figs. 6 and 7 show the results of the simultaneous and joint GSE inversion for $P = 7$ and $P = 5$, respectively. It can be seen that the fewer measurement lines (J) are applied the more the accuracy decreases.

In Fig. 8, we showed the results based on 21 measurement lines, applying Chebyshev polynomials of order $P = 7$. As it was shown in Fig. 5, the discretization error is almost negligible in this case, and therefore, Fig. 8 shows the effect of noise only.

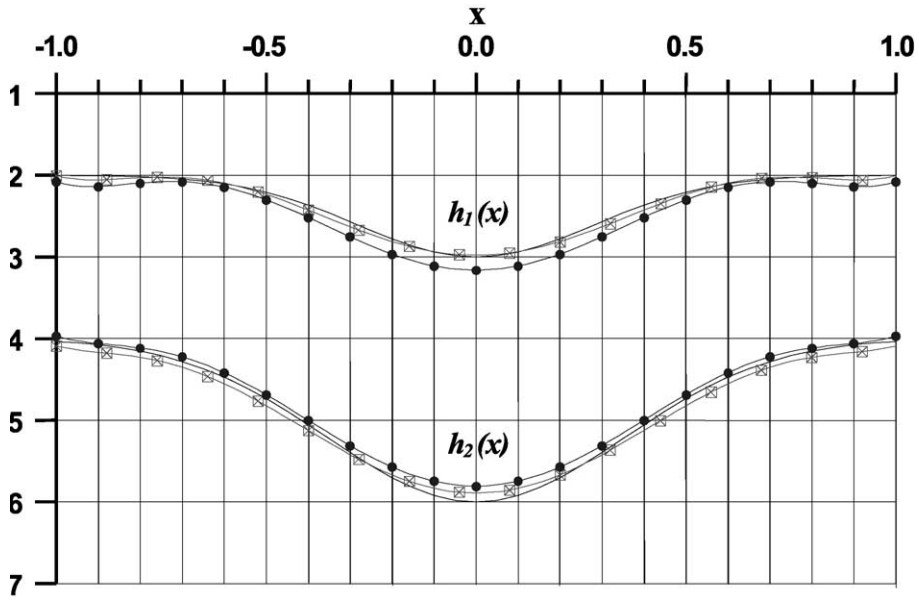

Fig. 8. The results of the simultaneous (rectangles) and joint (circles) GSE inversion based on Chebyshev polynomials ($J=21$, $P=7$).

The results show that the accuracy of joint GSE inversion increases approximately by a factor of 2 relative to the simultaneous inversion.

4. The resolution of geoelectric equivalence problem by means of GSE joint inversion

It is well known that the interpretation of DC geoelectric data has internal ambiguity and equivalence. This problem is well established in 1D geoelectric inversion (Koefoed, 1979). In order to resolve the equivalence problem, various kinds of geoelectric data were integrated in joint inversion algorithms (Raiche et al., 1985; Sharma and Kaikkonen, 1999). It was shown by Hering et al. (1995) that the internal ambiguities of the geoelectric method can efficiently be resolved by integrating seismic surface wave data. Carrying out the ambiguity and equivalence examinations also has a great importance for the GSE method.

The appearance of geoelectric equivalence has two basic types. In the first case, called *H*-type or conductive equivalence (Koefoed, 1979), a conductive layer is embedded between two more resistive layers ($\rho \ll \rho_{i-1}, \rho_{i+1}$). The sounding curves of two or more $H-$ type models of this kind can be equivalent if there is no difference in their lateral conductance ($S_i = h_i/\rho_i$), though the h_i and ρ_i parameters of the two or more structures can be completely different.

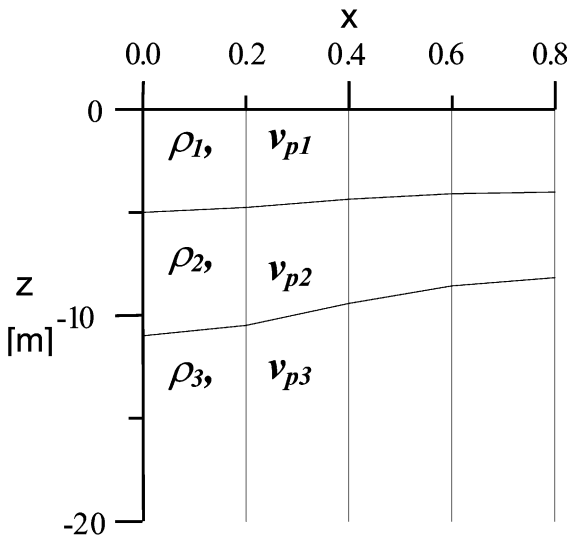

Fig. 9. The model (thickness functions) used for the simulated equivalence investigations.

Table 2

(a) The local values of the thickness functions at the five x coordinates chosen for the measurement layouts

	$x=0$	$x=0.2$	$x=0.4$	$x=0.6$	$x=0.8$
$h_1(x)$ [m]	5.000	4.779	4.368	4.105	4.018
$h_2(x)$ [m]	6.000	5.704	5.055	4.474	4.155

(b) Resistivities and longitudinal velocities of the layers, used for the simulated conductive equivalence investigations

ρ_i [Ω m]	v_{pi} [m/s]
200	700
10	1500
200	2200

If a resistive layer is embedded in the structure ($\rho \ll \rho_{i-1}, \rho_{i+1}$), the effect of this layer can be characterized by the transverse resistance $T_i = h_i \rho_i$. Similarly, the sounding curves of two or more K-type models (Koefoed, 1979) can be equivalent if their T_i are equivalent. This phenomenon can be called K-type or resistive equivalence.

In both cases, the difference between the equivalent layer structures cannot be interpreted using DC geoelectric measurements only. In the first case of equivalence when a single DC geoelectric inversion is carried out, only the lateral conductance (S_i), while in the second case, only the transverse resistance (T_i) may be determined. While there is a functional connection between the thickness and the resistivity of the equivalent layer, it is impossible to have enough information to separate these parameters, which are perfectly correlated by their product or ratio during the inversion.

For a unique separation, one needs a priori knowledge about either the resistivity or the thickness of the layer. In this section, the resolution of both types of equivalence phenomena will be investigated with the help of seismic refraction–DC geoelectric GSE joint

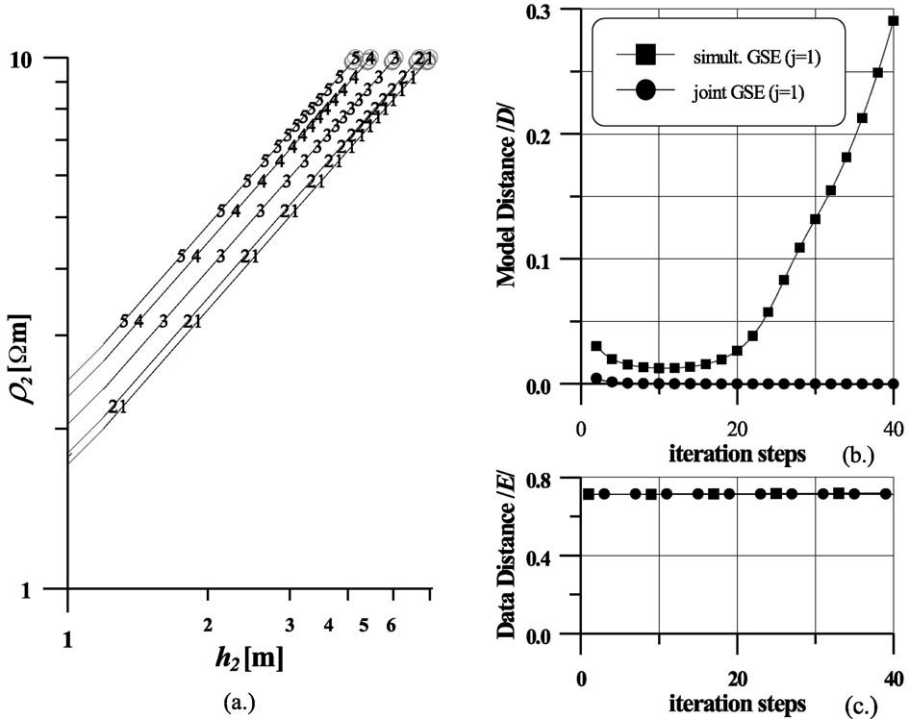

Fig. 10. (a–c) The results of the conductive equivalence investigations. (a) Functional connection between the thickness and resistivity of the second layer at the five measurement lines during the simultaneous (numbered lines, 1,. . .,5) and joint (circles) GSE inversion. (b) Model-and, (c) data distances during simultaneous (squares) and joint (circles) GSE inversion for the first measurement line ($j=1$).

inversion, in which the common thickness parameters can provide additional information to resolve the problematic parameters.

4.1. Resolution of conductive-type equivalence problem

In this investigation, an *H*-type model was defined (Fig. 9; Table 2a,b) and synthetic DC geoelectric and seismic refraction data sets were generated along five measurement profiles by using 2D and 3D finite difference forward codes with the x coordinates of {0, 0.2, 0.4, 0.6, 0.8}. The data are contaminated with 1% random (Gaussian) noise. The accuracy and reliability of parameter estimations were examined by the help of the simultaneous and joint GSE inversion using cell-wise constant base functions. Though the simultaneous geoelectric GSE inversion was started from the most favourable model (the exact model, shown in Table 2a,b), at either measurement line, a stable solution was not achieved. In Fig. 10a, the estimated parameters ρ_2 are presented in the function of the parameters h_2 during the iterations of the inversion with numbered solid lines (1,. . .,5) at the five measurement lines. Fig. 11 shows that the lateral conductance ($S_{2,j}=h_{2,j}/\rho_{2,j}$) remains constant during the iterations (j denotes the measurement lines, $j=1,...,5$). The curve shows functional connection between the estimated parameters $h_{2,j}-\rho_{2,j}$ during all steps of the inversion, which is proved by the value of the correlation between these parameters (CORR($h_{2,j},\rho_{2,j}$)=1). It means that in this case, the single inversion is able to determine the ratio of these parameters and it is impossible to resolve their correct values. At different measurement lines, the simultaneous geoelectric GSE inversion diverges along the functions $\rho_{2,j}=k_j h_{2,j}$, where the values of coefficient k_j are the reciprocal of the lateral conductances $S_{2,j}$. It is important to note that during the inversion, every point ($h_2-\rho_2$ combination) of the above functions

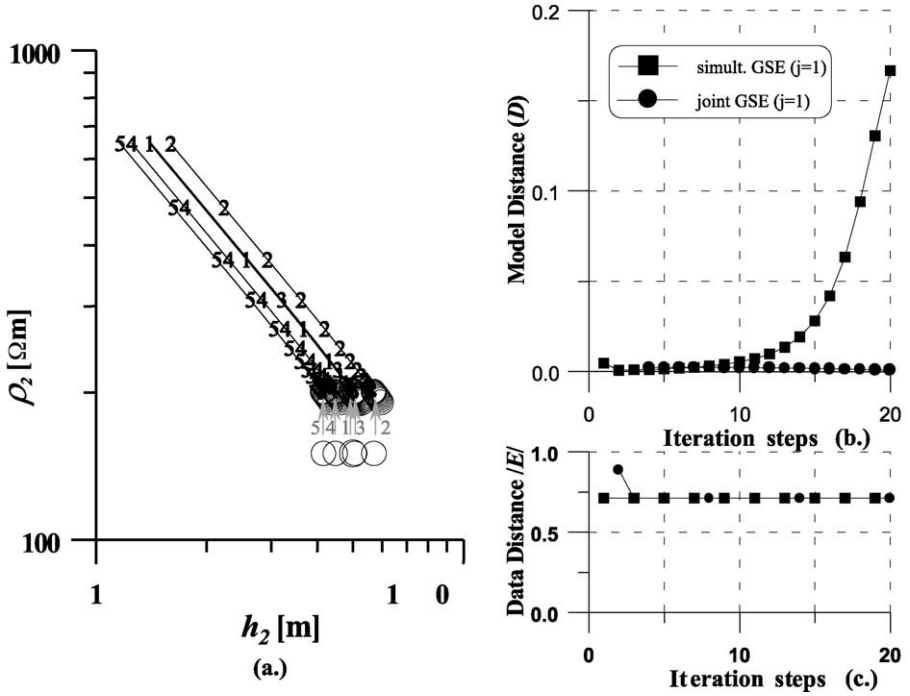

Fig. 11. The results of the resistive equivalence investigations. Functional connection between the thickness and resistivity of the second layer at the five measurement lines during the simultaneous (numbered lines, 1,. . .,5) and joint (circles) GSE inversion. The numbered arrows show the estimated parameter-combinations of the joint GSE inversion.

Table 3
Resistivities and longitudinal velocities of the layers, used for the resistive equivalence investigations

ρ_i [Ω m]	v_{pi} [m/s]
10	700
200	1500
10	2200

$\rho_{2,j}(h_{2,j})$ is a solution of the inversion in the sense that the fitting of the "observed" and calculated sounding curves characterized by the relative data distance (E) is the best (and equivalent) estimate at every point, though in the model space, the procedure diverges from the exact model, characterized by the model distance (D), which is continuously growing during the iterations of the inversion. Demonstrating this, the typical behaviour of the relative data distances (E) and model distances (D) are shown in Fig. 10b,c as a function of iteration steps by using the results of the first line ($j=1$).

After carrying out the seismic refraction–DC geoelectric joint GSE inversion (which was convergent), the equivalence interval became smaller at every line. One can see these results in Fig. 10 with circles. It is obvious that the joint inversion follows the same functions $\rho_{2,j}(h_{2,j})$, but the additional data set provides more information about $h_{2,j}$ ($j=1,\ldots,5$), and the inversion process converges to the exact values and reduces the equivalence intervals to a great extent. Furthermore, the correlation values become more

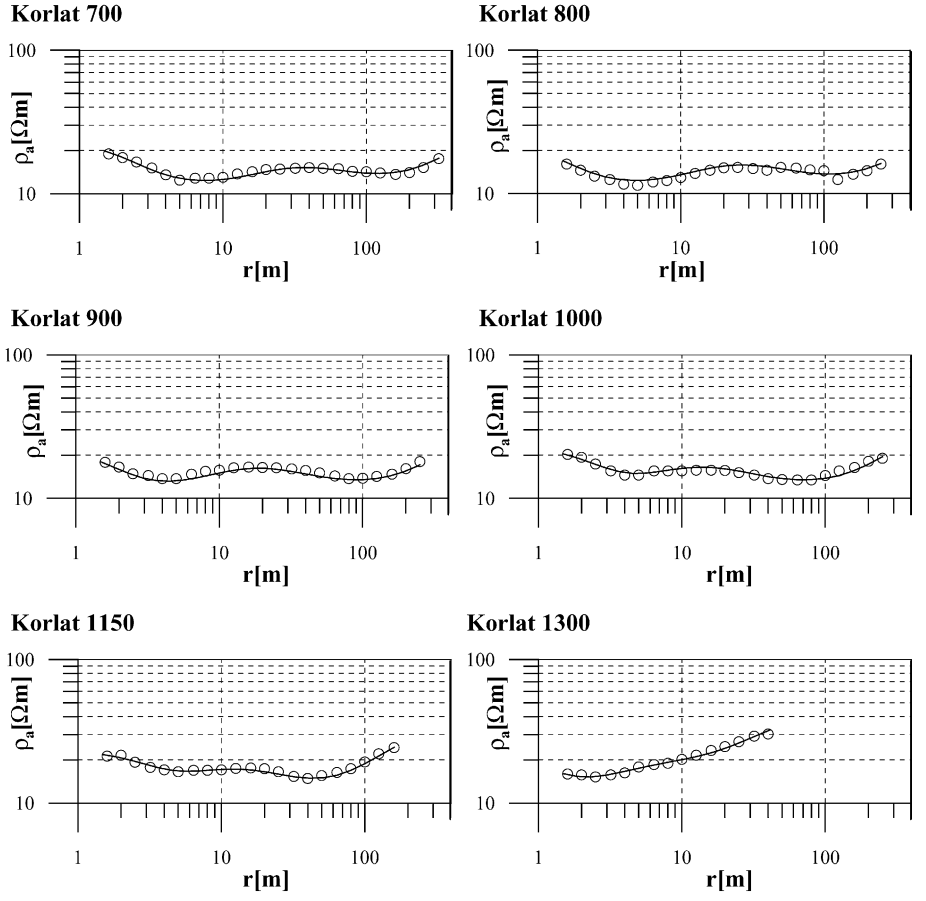

Fig. 12. The measured VES sounding curves (circles) and the fitted data (continuous lines) calculated from the model estimated by the simultaneous GSE inversion using Chebyshev polynomials. r denotes the half distance between current electrodes A and B.

favourable, the functional connections (maximal correlation) between $h_{2,j}$ and $\rho_{2,j}$ have disappeared.

Based on these results, it can be stated that the joint GSE inversion is capable to resolve the inherent geoelectric equivalence and to produce significantly narrower equivalence intervals.

4.2. Resolution of resistive-type equivalence problem

For these investigations, a *K*-type model was defined by the same thickness functions as presented in the previous section (Fig. 9; Table 2a) and by petrophysical parameters shown in Table 3. Similarly to the previous examinations, synthetic DC geoelectric and seismic refraction data sets were generated along the five measurement profiles, which are contaminated with 1% random noise.

We examined the accuracy and reliability of parameter estimation of the simultaneous geoelectric and the seismic refraction–DC geoelectric joint GSE inversion of these data sets. In Fig. 11. the estimates of $\rho_{2,j}$ are presented as a function of $h_{2,j}$ during the iterations at the five different measurement lines ($j=1,\ldots,5$). The numbered lines denote the results for the five measurement layouts of simultaneous geoelectric GSE inversion. These results are similar to those of the conductive equivalence investigations, with the difference that, in this case—as it can be seen in Fig. 11—the transverse resistances $T_{2,j}=h_{2,j}\rho_{2,j}$ of the second layer remain constant during the iterations, as the procedure diverges along the functions $\rho_{2,j}=T_{2,j}/h_{2,j}$. The correlation between the resistivity and thickness values of the second layer ($\mathrm{CORR}(h_{2,j},\rho_{2,j})=-1$) also shows the functional (hyperbolic) connection.

The estimates of the refracted-geoelectric joint GSE (started from a starting model with $\rho_{2,j}=150$ ($j=1,\ldots,5$)) are shown with circles for each layout in Fig. 11. The numbered arrows show the estimated parameter combinations of joint GSE inversion, which stabilized close to the exact values.

Based on the results we found, the joint GSE is successful in resolving the resistive-type equivalence, too.

5. Field results

The numeric experiments presented above show that the simultaneous GSE inversion method provides stable and reliable estimates. It was shown that, relative to the independent inversion of data from a single VES layout, the accuracy of the parameter estimation appreciably increases with the number of layouts integrated into the GSE simultaneous inversion. Because of this improvement in stability and

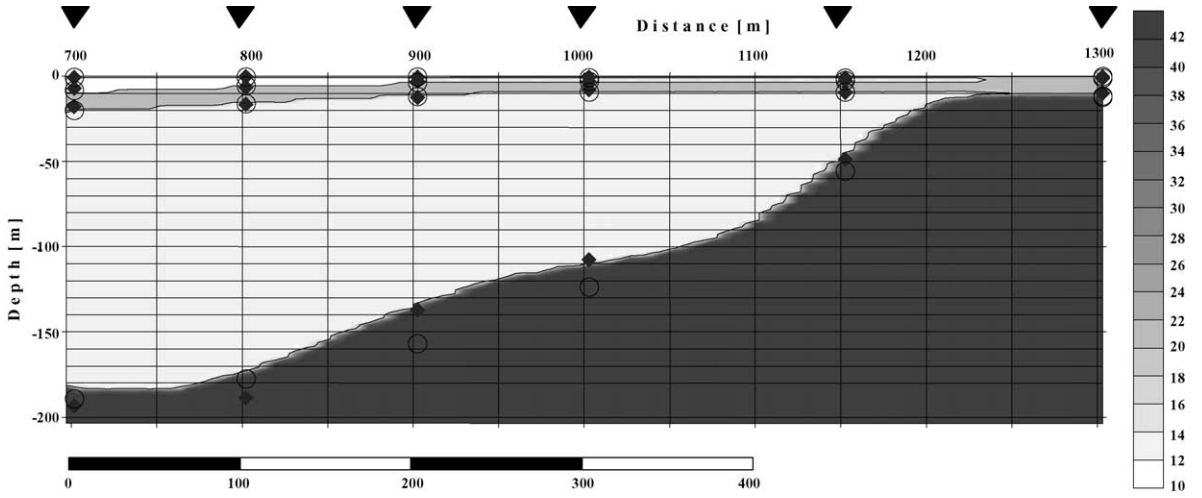

Fig. 13. The model resulting from the 1.5-D interpretation (after Gyulai and Ormos, 1997) and depths of layers below the measurement lines estimated by simultaneous GSE inversions using fifth-degree Chebyshev polynomial (circles) and interval-wise constant (rhombuses) base functions.

Table 4
The parameters of the starting model used in the simultaneous GSE inversion of field data

$h_i(x_1)$ [m]	$h_i(x_2)$ [m]	$h_i(x_3)$ [m]	$h_i(x_4)$ [m]	$h_i(x_5)$ [m]	$h_i(x_6)$ [m]	ρ_i [Ω m]
0.3	0.5	0.7	0.5	0.8	1.5	18.0
0.5	2.0	2.5	2.0	3.0	4.0	10.0
6.0	19.0	18.0	23.0	18.0	30.0	18.0
4.0	40.0	75.0	110.0	135.0	135.0	12.0
–	–	–	–	–	–	60.0

reliability, the GSE method can efficiently be applied in the interpretation of field data sets.

We used the simultaneous GSE to interpret the geoelectric VES data sets measured at the Hungarian village Korlat. The six measurement lines were aligned with the strike direction of the approximately 2D geologic structure. The measured sounding curves are presented in Fig. 12 by circles.

The data were previously interpreted by Gyulai and Ormos (1997) by using the 1.5D inversion method. The results of the 1.5D interpretation are shown in Fig. 13 together with the depth values calculated from the thickness functions estimated by GSE inversions based on Chebyshev polynomials and piecewise constant basis functions. It can be seen that there is a good agreement between the depth curves calculated by the 1.5D and the GSE inversion, the latter being derived independently.

The GSE inversion based on fifth-degree Chebyshev polynomials started from the initial model in Table 4 yields the parameters shown in Table 5. The close fitting ($E=3.4\%$) of the measured and calculated data can be seen in Fig. 12.

The data set was also interpreted by means of GSE based on interval-wise constant functions using the starting model given in Table 4. The results are shown in Table 6 and the corresponding depth values are shown in Fig. 13 (rhombuses). The relative distance between the measured and calculated data was $E=4.6\%$. It can be seen that the two results found by the simultaneous GSE method based on Chebyshev polynomials and interval-wise constant functions were in good agreement.

Table 5
The estimated parameters of GSE inversion based on Chebyshev polynomials

$h_i(x_1)$ [m]	$h_i(x_2)$ [m]	$h_i(x_3)$ [m]	$h_i(x_4)$ [m]	$h_i(x_5)$ [m]	$h_i(x_6)$ [m]	ρ_i [Ω m]
0.50	1.43	1.07	0.74	0.65	0.99	23.06
0.93	1.48	2.10	3.21	5.06	7.58	11.36
10.38	6.76	6.43	8.14	10.40	11.52	20.62
0.73	45.11	112.68	143.82	159.47	167.45	12.57
–	–	–	–	–	–	50.38

Table 6
The estimated parameters of GSE inversion based on interval-wise constant functions

$h_i(x_1)$ [m]	$h_i(x_2)$ [m]	$h_i(x_3)$ [m]	$h_i(x_4)$ [m]	$h_i(x_5)$ [m]	$h_i(x_6)$ [m]	ρ_i [Ω m]
0.54	1.37	1.07	0.79	0.60	1.00	23.4
0.97	1.48	2.22	2.62	6.14	6.34	11.0
8.76	7.07	4.97	9.16	9.98	10.61	18.9
0.20	38.5	98.5	123.4	170.2	173.9	12.5
–	–	–	–	–	–	36.7

6. Conclusions

A new joint inversion scheme for the interpretation of DC geoelectric and refraction seismic data measured above 2D geologic structure was introduced and analysed. The laterally varying model parameters were discretized by series expansion. In the approximate (1D) forward modelling, the integral mean of the functions describing the laterally varying model parameters were used. The data were assumed to be collected along various measurement lines laid out parallel with the strike direction of the 2D geologic model.

It was shown that the proposed Generalised Series Expansion (GSE) method results in a more stable and reliable parameter estimation, compared to the local (1D) inversion using only one data set collected along a single measurement line. This is valid for both cases of simultaneous and joint GSE inversion. It was also shown that the geoelectric equivalence problem (inherent in DC inversion) can be efficiently resolved by integrating refraction seismic data sets into the inversion in the framework of the joint GSE method.

Acknowledgements

The author is grateful to the editors (especially to Prof. N.B. Christensen) for their comments and the

criticisms, which helped to improve this paper. The presented investigations were partly carried out in the framework of a Roman Herzog Fellowship supported by the Alexander von Humboldt Foundation and in the framework of the OTKA Postdoctoral Fellowship of the Hungarian Scientific Research Fund (OTKA D 32836). The investigations were also aided by a project of the Deutsche Forschungsgemeinschaft (No. DR 110/8-1, 436 UNG 113/125) and the Hungarian Academy of Sciences (No. 30 008/70/96). The author is a member of the MTA—Miskolc University Research Group for "Geophysical Inversion and Tomography". I wish to express my thanks for the support and especially to Prof. M. Dobróka, Dr. Á. Gyulai, Dr.T. Ormos and Prof. L. Dresen for their useful advice and guide, and thanks are also due to Á. Gyulai, T. Ormos, E. Prácser and I. Török for providing the 2D and 3D forward modelling data and the field data.

References

Beard, L.P., Morgan, F.D., 1991. Assessment of 2-D structures using 1-D inversion. Geophysics 56 (6), 874–883.

Dobróka, M., 1994. Dispersion relation of Love-type waves propagating in an inhomogeneous seismic waveguide with varying thickness: inversion of the absorption–dispersion characteristics. Doctoral thesis, University of Miskolc, Hungary.

Dobróka, M., Gyulai, Á., Ormos, T., Csókás, J., Dresen, L., 1991. Joint inversion of seismic and geoelectric data recorded in an underground coal mine. Geophysical Prospecting 39, 643–665.

Dobróka, M., Kis, M., Turai, E., 2001. Generalised Series Expansion (GSE) method used in the joint inversion of MT and DC geoelectric data. Publication of the University of Miskolc, Series A, Mining, Geosciences 59, 39–51.

Gyulai, Á., 2000. New geoelectrical inversion process for the determination of geological structures: combined 2-D and 3-D function inversion. Magyar Geofizika 40 (4), 94–99.

Gyulai, Á., Ormos, T., 1997. Interpretation of vertical electrical sounding curves with 1.5-D inversion method. Magyar Geofizika 38, 25–36.

Gyulai, Á., Ormos, T., 1999. A new procedure for the interpretation of VES data: 1.5-D simultaneous inversion method. Journal of Applied Geophysics 41, 1–17.

Hering, A., Misiek, R., Gyulai, Á., Ormos, T., Dobróka, M., Dresen, L., 1995. A joint inversion algorithm to process geoelectric and surface wave seismic data. Geophysical Prospecting 43, 135–156.

Kis, M., 1996. Global optimization of geophysical data by the use of a simulated annealing algorithm. Magyar Geofizika 37, 170–181.

Kis, M., 1998. Investigation of near-surface structures by means of joint inversion of seismic and geoelectric data; 4. Global optimization of geophysical data using Simulated Annealing (pp. 51–73); 5. Investigation of 2D geologic structures by means of inversion using the series expansion method (pp. 73–99). PhD thesis, University of Miskolc, Hungary.

Kis, M., Dobróka, M., Amran, A., 1995. Joint inversion of geoelectric, refraction- and surface wave seismic data. 57th EAEG Meeting, Glasgow, 29 May–3 June.

Kis, M., Gyulai, Á., Ormos, T., Dobróka, M., Dresen, L., 1999. Grenzflächen-bestimmung von 2D Strukturen mit lokaler 1D Näherung (Interface-determination of 2D structures by locally 1D approximation). Proceedings of 59th DGG (Deutschen Geophysikalischen Gesellschaft) Meeting, Braunschweig, 8–12 March.

Kis, M., Gyulai, Á., Ormos, T., Dobróka, M., 2001. Joint inversion of Love and Rayleigh wave group velocities, refraction traveltimes and DC apparent resistivities measured above a 2D geological structure. Publication of the University of Miskolc, Series A, Mining, Geosciences 59, 23–39.

Koefoed, O., 1979. Geosounding Principles: 1. Resistivity Sounding Measurements Elsevier, Amsterdam.

Lines, L., Treitel, S., 1984. Tutorial: a review of least squares inversion and its application to geophysical problem. Geophysical Prospecting 32, 159–186.

Menke, W., 1984. Geophysical Data Analysis: Discrete Inverse Theory. Academic Press.

Morse, P.M., Feschbach, H., 1953. Methods of Theoretical Physics. McGraw-Hill, New York.

Ormos, T., Gyulai, Á., Kis, M., Dobróka, M., Dresen, L., 1998. A new approach for the investigation of 2D structures, method development and case history. 60th EAEG Meeting, Leipzig, 8–12 June.

Raiche, A.P., Jupp, D.L.B., Rutter, H., Vozoff, K., 1985. The joint use of coincident loop transient electromagnetic and Schlumberger sounding to resolve layered structures. Geophysics 50, 1618–1627.

Sharma, S.P., Kaikkonen, P., 1999. Appraisal of equivalence and suppression problems in 1D EM and DC measurements using global optimization and joint inversion. Geophysical Prospecting 47, 219–249.

Tarantola, A., 1987. Inverse Problem Theory, Methods of Data Fitting and Model Parameter Estimation Elsevier, Amsterdam.

Török, I., Kis, M., 2001. GSE and weighted GSE inversion in the interpretation of DC geoelectric data. Publication of the University of Miskolc, Series A, Mining, Geosciences 59, 63–75.

Yang, C.H., Tong, L.T., 1988. Joint inversion of DC, TEM and MT data. 58th Annual International SEG Meeting, Anaheim, 30 October–3 November.

Vozoff, K., Jupp, D.L.B., 1975. Joint inversion of geophysical data. Geophysical Journal of the Royal Astronomical Society 42, 977–991.